



HAL
open science

First Report of Electron Measurements During a Europa Footprint Tail Crossing by Juno

F. Allegrini, G. R. Gladstone, V. Hue, G. Clark, J. R. Szalay, W. S. Kurth, F. Bagenal, S. Bolton, J. E. P. Connerney, R. W. Ebert, et al.

► **To cite this version:**

F. Allegrini, G. R. Gladstone, V. Hue, G. Clark, J. R. Szalay, et al.. First Report of Electron Measurements During a Europa Footprint Tail Crossing by Juno. *Geophysical Research Letters*, 2020, 47, 10.1029/2020GL089732 . insu-03673124

HAL Id: insu-03673124

<https://insu.hal.science/insu-03673124>

Submitted on 24 Jun 2022

HAL is a multi-disciplinary open access archive for the deposit and dissemination of scientific research documents, whether they are published or not. The documents may come from teaching and research institutions in France or abroad, or from public or private research centers.

L'archive ouverte pluridisciplinaire **HAL**, est destinée au dépôt et à la diffusion de documents scientifiques de niveau recherche, publiés ou non, émanant des établissements d'enseignement et de recherche français ou étrangers, des laboratoires publics ou privés.

Copyright

Geophysical Research Letters

RESEARCH LETTER

10.1029/2020GL089732

Key Points:

- This is the first report of in situ electron measurements of a Europa footprint tail crossing
- Precipitating electron energies range from ~0.4 to ~25 keV with a characteristic energy of 3.6 keV, consistent with a low color ratio of the auroral emissions
- The instrument background caused by > ~5–10 MeV penetrating electrons increased during the crossing, opposite to what is observed at Io

Supporting Information:

- Supporting Information S1

Correspondence to:

F. Allegrini,
fallegrini@swri.edu

Citation:

Allegrini, F., Gladstone, G. R., Hue, V., Clark, G., Szalay, J. R., Kurth, W. S., et al. (2020). First report of electron measurements during a Europa footprint tail crossing by Juno. *Geophysical Research Letters*, 47, e2020GL089732. <https://doi.org/10.1029/2020GL089732>

Received 6 JUL 2020

Accepted 4 SEP 2020

Accepted article online 14 SEP 2020

First Report of Electron Measurements During a Europa Footprint Tail Crossing by Juno

F. Allegrini^{1,2} , G. R. Gladstone^{1,2} , V. Hue¹ , G. Clark³ , J. R. Szalay⁴ , W. S. Kurth⁵ , F. Bagenal⁶ , S. Bolton¹ , J. E. P. Connerney^{7,8} , R. W. Ebert^{1,2} , T. K. Greathouse¹ , G. B. Hospodarsky⁵ , M. Imai^{5,9} , P. Louarn¹⁰ , B. H. Mauk³ , D. J. McComas⁴ , J. Saur¹¹ , A. H. Sulaiman⁵ , P. W. Valek¹ , and R. J. Wilson⁶ 

¹Southwest Research Institute, San Antonio, TX, USA, ²Department of Physics and Astronomy, University of Texas at San Antonio, San Antonio, TX, USA, ³Johns Hopkins University Applied Physics Lab, Laurel, MD, USA, ⁴Department of Astrophysical Sciences, Princeton University, Princeton, NJ, USA, ⁵Department of Physics and Astronomy, University of Iowa, Iowa City, IA, USA, ⁶Laboratory for Atmospheric and Space Physics, University of Colorado Boulder, Boulder, CO, USA, ⁷Space Research Corporation, Annapolis, MD, USA, ⁸Goddard Space Flight Center, Greenbelt, MD, USA, ⁹Department of Electrical Engineering and Information Science, National Institute of Technology (KOSEN), Niihama College, Niihama, Japan, ¹⁰Institut de Recherche en Astrophysique et Planétologie (IRAP), Toulouse, France, ¹¹Institute of Geophysics and Meteorology, University of Cologne, Cologne, Germany

Abstract We report the first in situ observations of electron measurements at a Europa footprint tail (FPT) crossing in the auroral region. During its 12th science perijove pass, Juno crossed magnetic field lines connected to Europa's FPT. We find that electrons in the range ~0.4 to ~25 keV, with a characteristic energy of 3.6 ± 0.5 keV, precipitate into Jupiter's atmosphere to create the footprint aurora. The energy flux peaks at ~36 mW/m², while the peak ultraviolet (UV) brightness is estimated at 37 kR. We estimate the peak electron density and temperature to be 17.3 cm⁻³ and 1.8 ± 0.1 keV, respectively. Using magnetic flux shell mapping, we estimate that the radial width of the interaction at Europa's orbit spans roughly 3.6 ± 1.0 Europa radii. In contrast to typical Io FPT crossings, the instrument background caused by penetrating energetic radiation (> ~5–10 MeV electrons) increased during the Europa FPT crossing.

Plain Language Summary Jupiter's moons interact with Jupiter's space environment, or magnetosphere, and create auroral spots and tails in Jupiter's ionosphere. Io's aurora footprint on Jupiter is the strongest and most persistent of all moons, but Ganymede, Callisto, and Europa's auroral footprints are also routinely observed by remote platforms. NASA's Juno mission and its instrument suite occasionally fly through regions that are connected to the moon-magnetosphere interactions. During these crossings, Juno samples the electrons and ions that create the aurora. This paper is the first report of electron measurements taken during a Juno crossing of Europa's tail. These measurements confirm previous results based on remote observations. Most importantly, they provide a sample of the conditions in the regions associated with Europa's footprint aurora in Jupiter's magnetosphere.

1. Introduction

The interaction of the Jovian moons Io, Europa, Ganymede, and Callisto with the ambient plasma and fields leads to ultraviolet auroral emissions in the form of spots and tails in Jupiter's upper atmosphere (e.g., Bhattacharyya et al., 2018; Clarke et al., 2002; Grodent et al., 2006). Io's strong interaction creates the brightest spots of all and extends further downstream of the rotating plasma torus to form a weaker tail that gradually fades out. The interaction is thought to be mostly Alfvénic (e.g., Neubauer, 1998; Saur et al., 2013; Zarka, 2007), leading to broadband electron acceleration (e.g., Damiano et al., 2019; Hess et al., 2010; Saur et al., 2018; Sulaiman et al., 2020; Szalay et al., 2018, 2020, 2020a, 2020b), although other proposed acceleration mechanisms also suggest that the tail could be generated by quasi-static potential structures and current systems that transfer angular momentum from Jupiter to the Io plasma torus (e.g., Delamere et al., 2003; Ergun et al., 2009).

In recent in situ observations of the electron distributions during Io tail crossings (Szalay et al., 2018, 2020b), there were no signs of “inverted Vs” (signatures of potential structures) at the 1-s resolution of the JADE instrument. The distributions are broad in energy from ~0.1 to tens of keV and correlated with strong

electromagnetic wave signatures. Gershman et al. (2019) estimated that Alfvénic activity along the Io footprint tail (FPT) can provide up to $\sim 1,000$ mW/m² of Poynting flux close to the Io flux tube. Sulaiman et al. (2020) showed evidence of inertial Alfvén waves undergoing a turbulent cascade in concert with broadband bidirectional electron population, again suggesting Alfvénic acceleration of electrons. Ions are also accelerated, most likely from Alfvénic interactions, closer to Io (Szalay et al., 2020). And finally, the first report of in situ electron measurements during a Ganymede FPT crossing suggests that Alfvén waves accelerate the electrons that create the tail (Szalay et al., 2020a). This recent body of evidence supports the argument that Alfvénic acceleration sustains satellite FPTs.

The altitude of Io's main Alfvén wing (MAW; Bonfond et al., 2008) emission occurs at ~ 900 km above the limb (Bonfond, 2010) with a wide vertical extent (scale height of ~ 350 – 400 km), which points to broad electron energy distributions (Bonfond et al., 2009; Szalay et al., 2018). The vertical extent does not change with distance from the MAW (Bonfond, 2010). The color ratio, which is the ratio of unabsorbed UV intensity and absorbed UV intensity, provides a proxy for the penetration depth of the precipitating electrons at Jupiter (e.g., Gustin et al., 2002). Higher-energy electrons penetrate deeper into the atmosphere and are characterized by a higher color ratio. The color ratio of Io's footprint and tail is low compared to that of other auroral emissions (Gérard et al., 2014, 2016), implying that the mean electron energy is of the order of 1–2 keV.

Due to the difficulties in making observations, much less is known of the Europa footprint and tail. The Europa footprint is one of the weakest of the known footprints, and the tail is seldom visible and requires multiple remote observations carried out on a single day (Bonfond, Gladstone, et al., 2017; Grodent et al., 2006). The relative weakness of Europa's footprint is believed to be due to the lower Poynting flux generated by the interaction of Europa with the Jovian magnetosphere (Hess et al., 2011; Saur et al., 2013). Even from a close vantage point with the Ultraviolet Spectrometer (UVS; Gladstone et al., 2017) on Juno (Bolton et al., 2017), the Europa footprint and tail have been challenging to observe because they are weak and fall within patches of often much stronger other auroral emissions (Bonfond, Grodent, et al., 2017). From HST observations, Bonfond, Gladstone, et al. (2017) determined a mean FWHM of the Europa footprint of ~ 555 km (620 km in the south), which corresponds to about six times Europa's diameter when projected along the magnetic field lines at the equator. For reference, the plasma conditions at Europa are reviewed by Bagenal et al. (2015) while Bagenal and Dols (2020) review in situ and remote observations combined with models of the neutral and plasma populations from Io to Europa.

Here we report on the first in situ electron measurements during a crossing of the Europa FPT. The crossing occurred during the 12th science perijove in the north, when Juno's magnetic footprint mapped very close to that of Europa according to most recent magnetic field model JRM09 (Connerney et al., 2018). In section 2, we succinctly describe the instruments and data used in this study. We present the measurements in section 3, where we also list various parameters of the footprint crossing and of the electron distributions in a table. Section 4 provides a discussion of the results as well as a summary of our main results. These observations mostly confirm expectations from previous studies based on remote observations. One unexpected result, however, is the increase of penetrating radiation during the Europa FPT crossing, which is opposite to what is observed during an Io FPT crossing (Paranicas et al., 2019).

2. Brief Instruments Description

For this study we use in situ data from Juno's 12th perijove pass that occurred on 1 April 2018 or day of year (DOY) 91. We use data from five instruments (low- and high-energy electron spectrometers, magnetometer, UVS, and electromagnetic waves) that are briefly described in the following paragraphs.

The 0.05- to 100-keV electron distributions are measured at 1-s resolution by the Jovian Auroral Distributions Experiment-Electron (JADE-E), which consists of two identical top-hat electrostatic energy analyzers with a combined field of view (FOV) of 240° by 2 – 5.5° (McComas et al., 2017). The analyzers are equipped with deflectors to track the magnetic field direction that is broadcast every 2 s from the on-board magnetometer (MAG; Connerney et al., 2017). MAG consists of two independent magnetometer sensor suites with each a triaxial fluxgate magnetometer and collocated imaging sensors.

Over the course of the 1-s measurement, JADE-E steps 64 energies in an alternating pattern, going up in energy with the odd steps and down in energy with the even steps. Thus, it is possible to improve the

time resolution to 0.5 s by separating the up and down ramps as explained in Szalay et al. (2020b). We apply this method here since the Europa FPT crossing lasts only a few seconds. A background estimate for JADE-E is subtracted, and the intensities are calculated using an updated sensitivity equation both reported in Allegrini et al. (2020). However, JADE-E recorded very high count rates that exceeded a predefined threshold, which triggered a reduction of the detector gain. As a consequence, the background estimate and the sensitivity need to be corrected as explained in the supporting information.

The Juno Energetic particle Detector Instrument (JEDI; Mauk, Haggerty, Jaskulek, et al., 2017) measures electron distributions from ~ 25 keV to ~ 1 MeV in 24 logarithmically spaced energy channels. JEDI has three high-energy electron and ion sensors with fan-like FOVs. Two of the sensors (JEDI-90 and JEDI-270) have a similar FOV as JADE-E. Each sensor is composed of six electron and ion telescopes with an angular resolution of $\sim 9^\circ$ by 17° . Pitch angle distributions are calculated on the ground using the calibrated magnetic field vectors measured with Juno's magnetometer.

The Ultraviolet Spectrograph (UVS; Gladstone et al., 2017) is a photon-counting imaging spectrograph that measures ultraviolet emissions in the 68- to 210-nm range. The instrument slit is oriented parallel to Juno's spin axis, such that a 7° -wide swath is collected every spin. A flat scan mirror near the aperture allows shifting the look direction up to $\pm 30^\circ$ perpendicular to the spin plane, giving UVS the ability to target half of the sky at any given moment.

The Waves radio and plasma wave instrument (Kurth et al., 2017) measures one magnetic and one electric component of wave fields from 50 Hz to 20 kHz. It also measures electric fields at frequencies up to 41 MHz. For this paper, the most relevant measurements are burst mode electric waveforms in the frequency range of 10–150 kHz with a sample rate of 375 ksps. Each waveform capture includes 6,144 samples obtained over 16.4 ms once per second.

3. Results

Figure 1 shows an overview of Juno's perijove 12 North pass where we indicate features such as the main oval (from $\sim 09:06:52$ to $\sim 09:08:23$) and satellite FPTs. Over this period the Juno spacecraft descended from a joventric distance of $R = 1.80$ to $1.29 R_J$ (where $1 R_J = 71,492$ km), which corresponds to jovigraphic altitudes of $62 \cdot 10^3$ to $25 \cdot 10^3$ km above the 1-bar level. Figure 1a is a reconstructed UV image in false color. The red emissions come from deeper in the atmosphere whereas the white emissions are from higher altitudes. The brightness of the features is related to the integrated UV brightness. The main oval and Europa and Io's tails are indicated. Juno's magnetic footprint track was mapped onto this image using JRM09 (Connerney et al., 2018) with a current sheet model (Connerney et al., 1981, hereafter abbreviated CAN1981). The magnetic flux shells of Juno's trajectory mapped with this nondipolar magnetic field (labeled M -shell with the jovigraphic distance of the farthest point along the flux tube) ranged from $M = 53$ to 5 over this period. The thicker, light blue part of the track corresponds to the time period of this image's acquisition ($09:00:23$ to $09:15:23$). Using the same mapping, the locations of the field lines connected to the moons' M -shells is shown, with the dot being at the beginning of the image acquisition ($09:00:23$). There are discrepancies between the features of the UV image associated with the FPTs and the predicted locations. For example, the predicted crossing of Europa FPT is after $09:15$, but the Europa FPT aurora is mapped before $09:15$. A similar discrepancy is also seen for Io's FPT. A number of reasons likely account for those discrepancies. First, the mapping in this region is affected by a magnetic anomaly (Grodent et al., 2008). Second, our simple magnetic field mapping does not capture the local deformations in the magnetic field induced by the MAW (e.g., Szalay et al., 2020b). The brightest spot is typically not collocated with where the field line connected to the moon is (e.g., Hinton et al., 2019). Third, if the current from the CAN1981 current sheet model is stronger than the actual current, then Europa's FPT tends to move toward the magnetic equator. And fourth, a projection effect may exacerbate the discrepancies if the altitude of the emission does not correspond to the mapped altitude.

Figure 1b shows the combined electron energy spectrogram measured by JADE and JEDI, spanning an energy range from 50 eV to 1 MeV. The Io tail crossing is prominent, occurring shortly before $09:21$. On this time scale, however, the Europa FPT crossing is barely noticeable at $\sim 09:15:45$.

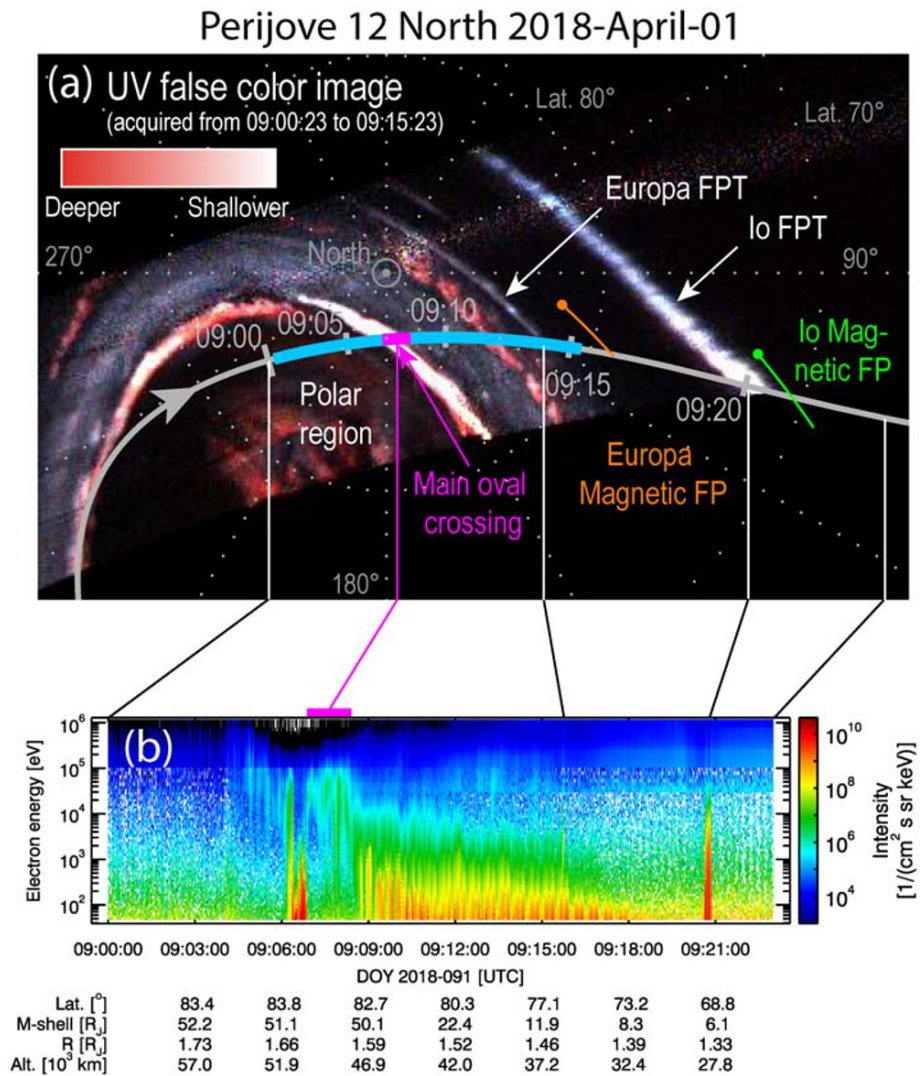


Figure 1. (a) UVS reconstructed false color image acquired from 09:00:23 to 09:15:23. The color is related to the depth of the emission where red comes from deeper in the atmosphere. Juno's magnetic footprint track is shown in gray and in light blue during the image acquisition. Europa and Io's magnetic footprints are shown in orange and green, respectively, using JRM09 + CAN1981. (b) Combined JADE and JEDI electron energy spectrogram from 50 eV to 1 MeV. The spacecraft jovigraphic latitude, M -shell, radial distance, and altitude above the 1-bar level are indicated below panel (a). The lines between the panels connect the features from the image (not the magnetic footprints) in panel (a) to their corresponding electron measurements in panel (b). There are discrepancies between the crossing times of the mapped UV features and the corresponding signatures in the electron data. For example, the Europa tail crossing in panel (a) occurs before 09:15 but is measured in the electrons after 09:15. More details are found in the text.

Figure 2 shows 90 s of JADE, JEDI, Waves, and UVS measurements zoomed in around the Europa FPT crossing, which occurred between $\sim 09:15:42$ and $\sim 09:15:45.5$, and is delimited by the thin vertical black lines. Figure 2a shows the energy spectrogram of the combined JADE and JEDI electron data averaged over look directions (Allegrini et al., 2020).

Figure 2b shows the spectrum of plasma waves between 10 and 80 kHz. The most obvious feature is whistler mode hiss with a sharp upper-frequency cutoff at about 35 kHz. Most pertinent to this work is the brief burst of intense narrowband emissions just above this cutoff at about 09:15:43, coincident with the Europa FPT crossing. Given the field-aligned electrons, it is likely these are electron plasma oscillations driven by a beam instability at 37.4 kHz, which we take as the electron plasma frequency f_{pe} . Since the electron density $n_e = (f_{pe}/8980)^{1/2}$, n_e is measured to be 17.3 cm^{-3} . We note that the

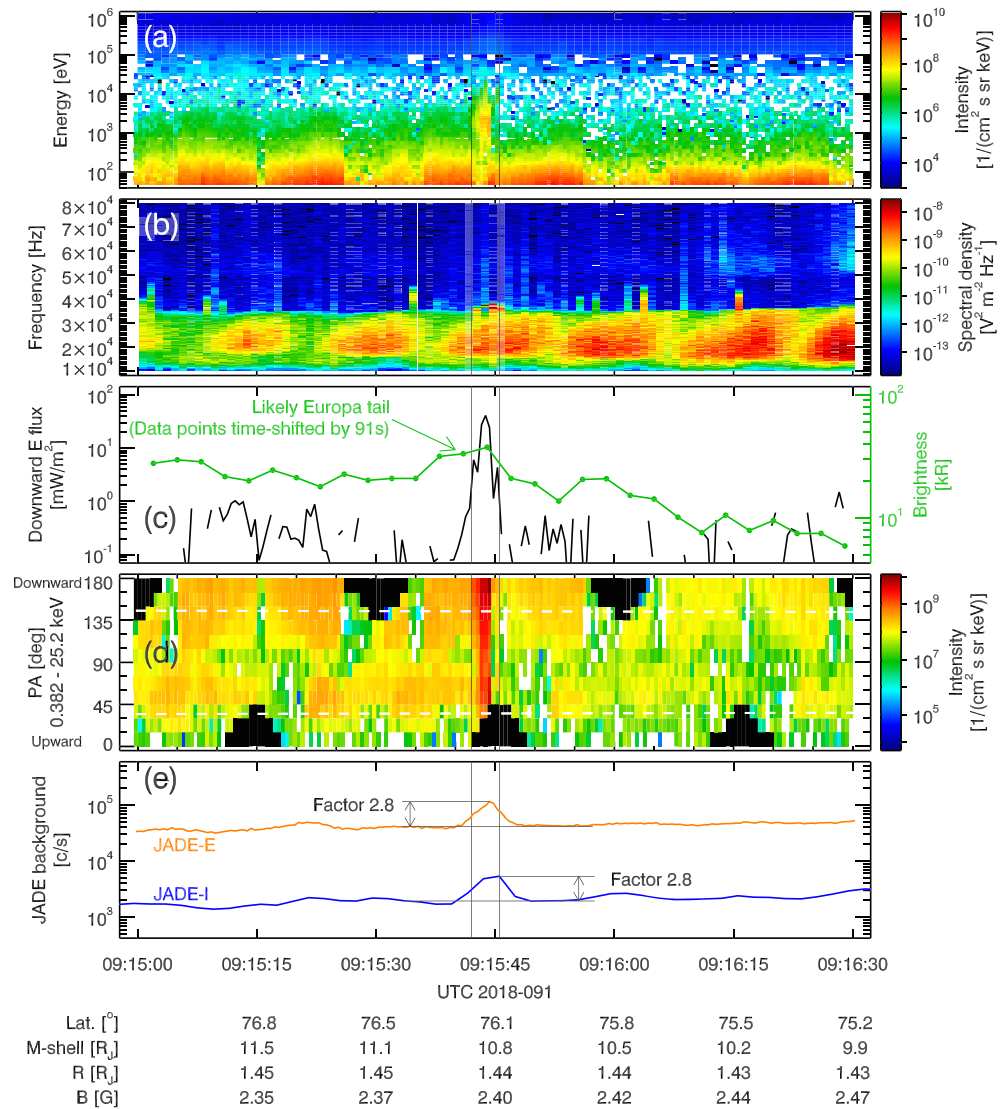


Figure 2. (a) Combined JADE and JEDI electron energy spectrogram showing the crossing of the Europa tail (~09:15:42 to ~09:15:45.5). (b) Plasma waves spectrum between 10 and 80 kHz showing a whistler mode hiss with a sharp upper-frequency cutoff at about 35 kHz during the crossing. (c) Downward (going toward Jupiter) electron energy flux in the loss cone (~35°) for electrons from ~0.382 to 25.2 keV and UV brightness (in green) time shifted to match the electron energy flux peak with the feature in Figure 1a. (d) Pitch angle spectrogram for electrons between ~0.382 and ~25.2 keV. The white dashed lines show an estimate of the loss cone angle, ~35° from the field. (e) JADE (-E for electron and -I for ion sensor) backgrounds due to radiation that penetrates through the instrument material and creates a signal. The jovigraphic latitude, *M*-shell (JRM09 + CAN1981), radial distance, and magnetic field strength are given at the bottom.

whistler mode cannot propagate above the lower of f_{pe} or f_{ce} , where f_{ce} is the electron cyclotron frequency. Since f_{ce} is 6.72 MHz at this time, the cutoff is almost certainly at or very close to f_{pe} , consistent with the frequency of the plasma oscillations.

Figure 2c shows the downward energy flux for 0.382 to 25.2 keV electrons that are within the loss cone (LC), which we estimate using the simple relationship LC angle $\approx \sin^{-1}(1/R^3)^{1/2}$ (Mauk, Haggerty, Paranicas, Clark, Kollmann, Rymer, Mitchell, et al., 2017a), where R is the jovicentric distance in R_J . The LC angle is about 35° at the time of the crossing. The green data points are estimates of the UV brightness at Juno’s magnetic footprint measured between 155 and 162 nm and multiplied by 8.1 to reflect for the total brightness emitted in the total H2 Lyman and Werner band systems (~80 to ~170 nm; Gérard et al., 2019; Gustin et al., 2013). We calculate the average UV brightness in a 0.1° radius around Juno’s magnetic footprint

(which corresponds to a radius of ~ 55 km for this time), in a similar manner as in Allegrini et al. (2020). By using the electron energy flux, Figure 1a, and the derived UV brightness, we determined that a time shift of 91 s of the derived UV brightness data was necessary to match the brightness of Europa's tail and other nearby UV features with the electron observations. The peak UV brightness associated with the FPT crossing is 37 kR.

Figure 2d shows a pitch angle spectrogram for ~ 0.382 – 25.2 keV electrons. The white dashed lines show the $\sim 35^\circ$ LC angle. The downward (upward) LC in this 90-s interval tends to be full (depleted), which is typical of that region (Allegrini et al., 2017, 2020).

Figure 2e shows the JADE-E and JADE-I (for Ions) backgrounds. The cause for the background comes from radiation that is sufficiently energetic to penetrate through the material of the instrument, create secondary particles, and trigger a signal in the detectors. The most likely candidates are energetic electrons above ~ 5 – 10 MeV. The background increased by a factor of 2.8 during Europa's FPT crossing. This could be due to either an increase in energetic particle flux, or a change in the spectrum, or a combination of both. Interestingly, a decrease in the penetrating background is observed during an Io FPT crossing as shown in Paranicas et al. (2019). They present strong evidence that wave-particle interactions are responsible for the decrease at Io's *M*-shells. It is not obvious what would cause such differences between Europa and Io's FPT crossing.

Figure 3 shows energy spectra (a) and pitch angle distributions (b) one spin (30 s) before (orange), one spin after (green), and during (black) the Europa FPT crossing. The data taken one spin before or after provide a baseline to highlight the changes during the crossing. The differences in the spectra between the baseline and during the crossing define the electron population that (1) causes the tail in the UV auroral emissions and (2) is in the flux tube connected to the Europa FPT.

Figure 3a shows that electrons between ~ 0.38 and ~ 25 keV are enhanced with respect to the baseline prior and post the FPT crossing. The jagged appearance of the spectra is due to rapidly (< 1 s) changing distributions.

In the case of Io, similar enhancements are seen from below the lowest energy measured (i.e., 100 eV up to PJ6 and 50 eV from PJ7 on) up to about 5 to 20 keV (Szalay et al., 2018). For PJ12N, however, enhancements up to ~ 50 keV were observed when Juno crossed the flux tube associated with the MAW (Szalay et al., 2020b).

In Figure 3b, we show the pitch angle distributions for electrons in the energy range of the enhancement seen in Figure 3a. Apart from a flux enhancement of a factor of ~ 12 for all pitch angles (with respect to one spin before), the distribution is not much different between the baseline and the crossing. The modest enhancement of a factor of ~ 2.4 between pitch angle of $\sim 142.5^\circ$ (third point from the right) and pitch angle 172.5° (first point on the right) could be an angle beam. The dip around pitch angle 90° is caused by spacecraft shadowing that has not yet been corrected. The gray data points correspond to pitch angles where JADE-E did not have full pitch angle FOV during the FPT crossing (see black pixels near pitch angle 0 in Figure 2d). The presence of a depleted upward LC during the crossing is disputable since JADE-E's FOV barely covered this part of the pitch angle distribution. However, as mentioned above, this region is usually characterized with a depleted upward LC, and it is probably safe to assume that the same occurs during the crossing of the Europa FPT.

Figure 3c shows an energy spectrogram at 0.5-s time resolution zoomed in on the FPT crossing, which is indicated between the two vertical black lines. Each half-second sample is color-coded (top of panel) for the curves shown in Figures 3d and 3e. Figure 3d shows the intensity during the FPT crossing. The distribution is broad in energy, but the spectrum also has a positive slope of about E^1 , which means that the phase space density (PSD) is flat in that region (Figure 3e). An energy beam resulting from coherent acceleration by an electrostatic potential would appear with a positive slope in PSD and a slope greater than 1 in intensity. Such beams have been identified in the auroral region at Jupiter by Mauk, Haggerty, Paranicas, Clark, Kollmann, Rymer, Bolton, et al. (2017b), and they tend to be sharply defined. On the contrary at Earth, the inverted-V electron distribution PSDs are relatively flat (e.g., Amm et al., 2002) with at most a small enhancement. A positive slope in PSD can indicate distributions unstable to wave growth, and wave-particle interactions tend to flatten the distribution. Therefore, it is plausible that the electron

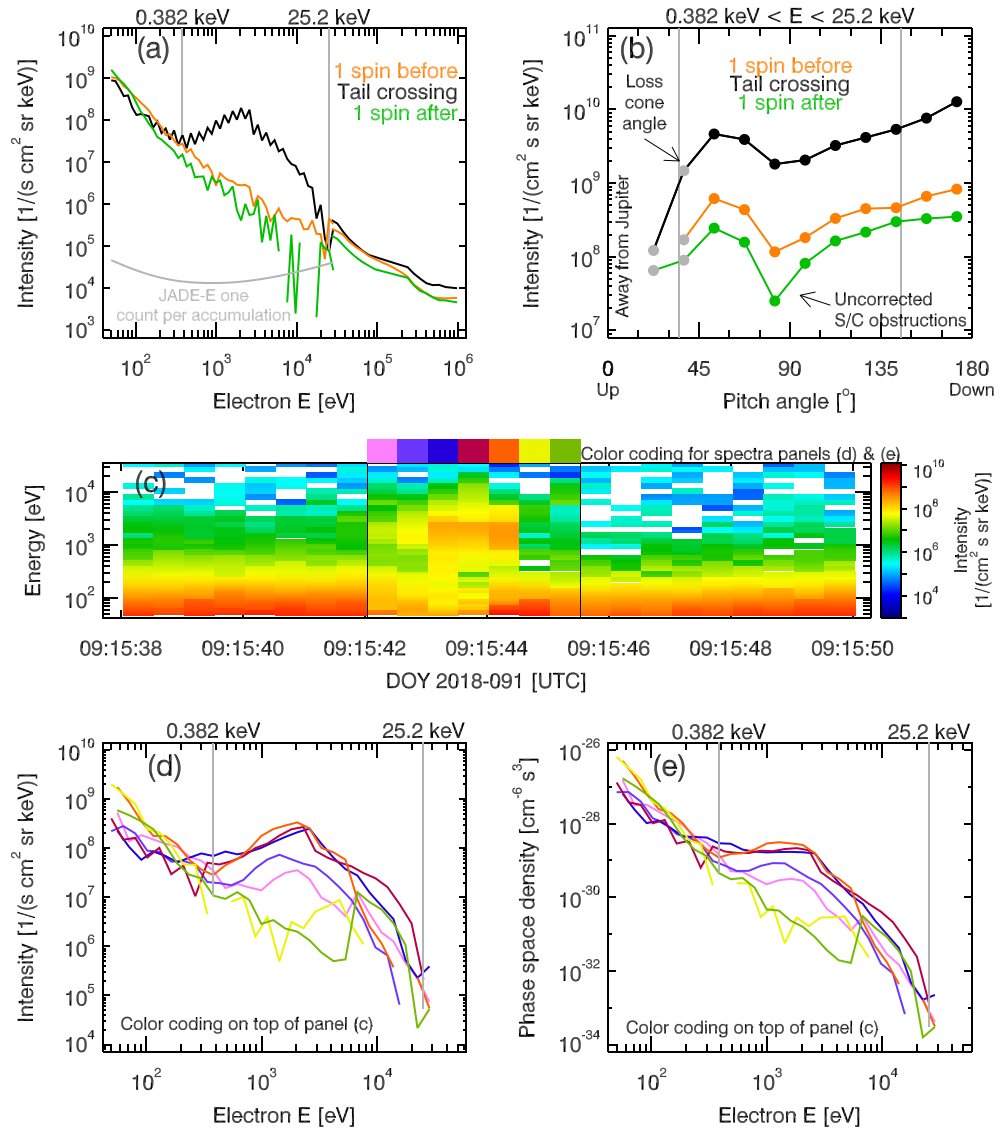


Figure 3. (a) Differential number flux (or intensity) as a function of energy during the Europa FPT crossing (black) and one spacecraft spin before (orange) and after (green). (b) Corresponding pitch angle distributions for 0.382 to 25.2 keV electrons. The gray data points correspond to pitch angles when JADE-E did not have full pitch angle field of view during the full time interval (see black “triangles” in Figure 2d). (c) Energy spectrogram zoomed in on the Europa FPT crossing. (d and e) The intensities and phase space densities during the crossing. The color coding is indicated on top of panel (c).

distributions from the Europa FPT crossing were accelerated at least in part by electrostatic acceleration, given this comparison with Earth auroral electron distributions. While no clear signs of “inverted Vs” were observed for the Io FPT crossings, there are two cases (PJ5N and PJ6N; Szalay et al., 2018) where the spectral slope is about 1, similar to this Europa FPT crossing.

To estimate the tail width at the equator, we simply use the change in M -shell during the time of the crossing and convert it to km. The crossing lasts for ~ 3.5 s (see vertical black lines in Figure 2), and the M -shell changes from ~ 10.864 to 10.785 , corresponding to a radial distance of $\sim 5.6 \cdot 10^3$ km or $3.6 R_{Eu}$ ($R_{Eu} = 1,560.8$ km = Europa radius). The main uncertainty comes from the duration of the crossing, and if we assume it to be ± 1 s, then the uncertainty of the radial extent of the tail at the equator is roughly $3.6 \pm 1.0 R_{Eu}$. This is consistent with an estimate of the size of the interaction region at the equator from Bonfond, Gladstone, et al. (2017) of $< 6 R_{Eu}$, considering that their estimate is based on the main spot

size and that the electron measurements presented here may have been connected to the tail and not necessarily to the main spot. An extent of approximately $3.6 R_{Eu}$ corresponds to approximately the size of the interaction region at Europa generating the Alfvén wings (e.g., Saur et al., 1998) and indicates that the tail is not widening. We can also compare the observed peak energy fluxes of $\sim 36 \text{ mW m}^{-2}$ with the Poynting flux in Europa's MAW, which is the primary energy supply. Based on estimates in Saur et al. (2013), the maximum Poynting fluxes lie in the range of 15 to 9,000 mW m^{-2} depending on Europa's position in the plasma sheet. Thus, only a small fraction of the maximum total electromagnetic energy flux is needed to power the electrons observed here.

Table S2 summarizes some of the parameters of the Europa FPT crossing. The energy flux (36 mW/m^2) and the characteristic energy (3.6 keV) are derived using Equations 1 and 2 in Allegrini et al. (2020). We limited the range of the integrals to 0.382 to 25.2 keV. Including energies lower than 0.382 would increase the energy flux by $<0.2\%$. The peak electron density (17.3 cm^{-3}) is derived from the electron plasma frequency (see above). The peak electron temperature (1.8 keV) is derived from numerical integrations of the JADE electron measurements.

For comparison, the peak energy flux for Io FPT crossings ranges from $\sim 0.25 \text{ mW/m}^2$ up to $\sim 580 \text{ mW/m}^2$ —when Juno crossed the flux tube of the MAW—and it decreases exponentially with the angular separation along Io's orbit between Io and the path taken by Alfvén waves from Io's orbit to Juno (Szalay et al., 2020b).

4. Discussion and Conclusion

The UV brightness peak that we associate with the Europa tail crossing is mapped about 91 s prior to the crossing registered by JADE and JEDI. A time shift in the same direction also makes the UV brightness associated with the main oval crossing and the Io FPT crossing qualitatively match the energy flux from JEDI and JADE better. Thus, it is likely that the shift reflects mapping inaccuracies. The ratio between the peak brightness and the energy flux is $37/36 \approx 1 \text{ kR}/(\text{mW/m}^2)$. It is well below the usual rule of thumb of $10 \text{ kR}/(\text{mW/m}^2)$ (Gustin et al., 2016). However, it should be noted that the rule of thumb is suggested for 70–140 keV electrons, which is about an order of magnitude higher than the energy of interest here. Still, it seems that there is a discrepancy that could be due to the following reasons. The UV brightness presented in this study was derived using a successive amount of coadded swaths recorded over the course of 15 min. The Europa FPT on the image (Figure 1a) was not imaged when Juno was magnetically connected to that feature ($\sim 09:15:45$), but ~ 400 s on average before the crossing. Therefore, it is likely that the portion of the tail used to calculate the UV brightness was different than the tail where Juno crossed. As shown in Figure 1a, Europa's magnetic footprint moves during the image acquisition (15 min = 900 s). Another possibility is that the conversion from electron energy flux to UV brightness is not very efficient. However, this would be a significant departure from the expectation at higher energies.

We reported on electron measurements of a flux tube connected to the Europa FPT or MAW spot aurora. The crossing occurred at a joventric radial distance of $1.44 R_J$ (altitude $36 \cdot 10^3 \text{ km}$ above the 1 bar level). In summary,

1. the electron energy is in the range from ~ 0.4 to ~ 25 keV, with a characteristic energy of 3.6 keV, consistent with the low color ratio of satellite footprint emissions (Gérard et al., 2014, 2016);
2. the distribution is broad in energy, but the spectrum also has a positive slope of about E^1 . Due to similarities with “inverted V” electron distributions observed at Earth, it is possible that the electron distributions from the Europa FPT crossing were accelerated at least in part by electrostatic acceleration;
3. the energy flux of the precipitating electrons peaks at 36 mW/m^2 . The estimated peak UV brightness is $\sim 37 \text{ kR}$, which is consistent with previous observations (Grodent et al., 2006). The ratio between the peak brightness and the energy flux is $\sim 1 \text{ kR}/(\text{mW/m}^2)$, which is well below the usual rule of thumb of $10 \text{ kR}/(\text{mW/m}^2)$ for 70–140 keV electrons (Gustin et al., 2016);
4. the electron density is 17.3 cm^{-3} , and the electron temperature is $1.8 \pm 0.1 \text{ keV}$;
5. the estimated size of the interaction region at Europa's orbit is approximately 3.6 ± 1.0 Europa radii;
6. the JADE instrument background caused by penetrating radiation (likely $> \sim 5\text{--}10 \text{ MeV}$ electrons) increased during the crossing by a factor of ~ 2.8 above ambient. This is opposite to what is observed at Io (e.g., Paranicas et al., 2019); and

7. this Europa and the numerous Io FPT crossings show a lot of similarities. However, there are noteworthy differences such as the enhancements in the spectra that extend to lower energies (below the minimum measured energy by JADE-E, i.e., 100 or 50 eV) for Io. Also, only 2 out of 18 reported crossings of the Io FPT (PJ5N and PJ6N) show a positive slope of about E^1 similar to that of the Europa spectra shown here.

We anticipate several more crossings by Juno of the Europa flux shells, especially if the mission is extended beyond the prime phase.

Data Availability Statement

The data presented here reside at NASA's Planetary Data System (<https://pds-ppi.igpp.ucla.edu/mission/JUNO>), and we used the following data sets: JNO-J_SW-JAD-3-CALIBRATED-V1.0, JNO-J-JED-3-CDR-V1.0, JNO-E/J/SS-WAV-3-CDR-SRVFULL-V1.0, and JNO-J-3-FGM-CAL-V1.0. The data from the figures is publicly available on a permanent repository (at the following address: <https://doi.org/10.5281/zenodo.3997252>).

Acknowledgments

We thank all the outstanding women and men who have made Juno and the instrument suite so successful. This work was funded by the NASA New Frontiers Program for Juno, at the University of Iowa through Contract 699041X, at the University of Colorado through Contract 699050X, and at Princeton University through Contract NNM06AA75C with the Southwest Research Institute.

References

- Allegrini, F., Bagenal, F., Bolton, S., Connerney, J., Clark, G., Ebert, R. W., et al. (2017). Electron beams and loss cones in the auroral regions of Jupiter. *Geophysical Research Letters*, *44*, 7131–7139. <https://doi.org/10.1002/2017GL073180>
- Allegrini, F., Mauk, B., Clark, G., Gladstone, G. R., Hue, V., Kurth, W. S., et al. (2020). Energy flux and characteristic energy of electrons over Jupiter's main auroral emission. *Journal of Geophysical Research: Space Physics*, *125*, e2019JA027693. <https://doi.org/10.1029/2019JA027693>
- Amm, O., Birn, J., Bonnell, J., Borovsky, J. E., Carbary, J. F., Carlson, C. W., et al. (2002). Chapter 4—In situ measurements in the auroral plasma. *Space Science Reviews*, *103*(1/4), 93–208. <https://doi.org/10.1023/A:1023082700768>
- Bagenal, F., & Dols, V. (2020). The space environment of Io and Europa. *Journal of Geophysical Research: Space Physics*, *125*, e2019JA027485. <https://doi.org/10.1029/2019JA027485>
- Bagenal, F., Sidrow, E., Wilson, R. J., Cassidy, T. A., Dols, V., Cray, F. J., et al. (2015). Plasma conditions at Europa's orbit. *Icarus*, *261*, 1–13. <https://doi.org/10.1016/j.icarus.2015.07.036>
- Bhattacharyya, D., Clarke, J. T., Montgomery, J., Bonfond, B., Gérard, J. C., & Grodent, D. (2018). Evidence for auroral emissions from Callisto's footprint in HST UV images. *Journal of Geophysical Research: Space Physics*, *123*, 364–373. <https://doi.org/10.1002/2017JA024791>
- Bolton, S. J., Lunine, J., Stevenson, D., Connerney, J. E. P., Levin, S., Owen, T. C., et al. (2017). The Juno Mission. *Space Science Reviews*, *213*(1–4), 5–37. <https://doi.org/10.1007/s11214-017-0429-6>
- Bonfond, B. (2010). The 3-D extent of the Io UV footprint on Jupiter. *Journal of Geophysical Research*, *115*, A09217. <https://doi.org/10.1029/2010JA015475>
- Bonfond, B., Gladstone, G. R., Grodent, D., Greathouse, T. K., Versteeg, M. H., Hue, V., et al. (2017). Morphology of the UV aurorae Jupiter during Juno's first perijove observations. *Geophysical Research Letters*, *44*, 4463–4471. <https://doi.org/10.1002/2017GL073114>
- Bonfond, B., Grodent, D., Badman, S. V., Saur, J., Gérard, J. C., & Radioti, A. (2017). Similarity of the Jovian satellite footprints: Spots multiplicity and dynamics. *Icarus*, *292*, 208–217. <https://doi.org/10.1016/j.icarus.2017.01.009>
- Bonfond, B., Grodent, D., Gérard, J. C., Radioti, A., Dols, V., Delamere, P. A., & Clarke, J. T. (2009). The Io UV footprint: Location, inter-spot distances and tail vertical extent. *Journal of Geophysical Research*, *114*, A07224. <https://doi.org/10.1029/2009JA014312>
- Bonfond, B., Grodent, D., Gérard, J. C., Radioti, A., Saur, J., & Jacobsen, S. (2008). UV Io footprint leading spot: A key feature for understanding the UV Io footprint multiplicity? *Geophysical Research Letters*, *35*, L05107. <https://doi.org/10.1029/2007GL032418>
- Clarke, J. T., Ajello, J., Ballester, G., Jaffel, L. B., Connerney, J., Gérard, J. C., et al. (2002). Ultraviolet emissions from the magnetic footprints of Io, Ganymede and Europa on Jupiter. *Nature*, *415*(6875), 997–1000. <https://doi.org/10.1038/415997a>
- Connerney, J. E. P., Acuña, M. H., & Ness, N. F. (1981). Modeling the Jovian current sheet and inner magnetosphere. *Journal of Geophysical Research*, *86*(A10), 8370–8384. <https://doi.org/10.1029/JA086ia10p08370>
- Connerney, J. E. P., Bann, M., Bjarno, J. B., Denver, T., Espley, J., Jorgensen, J. L., et al. (2017). The Juno magnetic field investigation. *Space Science Reviews*, *213*(1–4), 39–138. <https://doi.org/10.1007/s11214-017-0334-z>
- Connerney, J. E. P., Kotsiaros, S., Oliverson, R. J., Espley, J. R., Joergensen, J. L., Joergensen, P. S., et al. (2018). A new model of Jupiter's magnetic field from Juno's first nine orbits, 2590–2596. *Geophysical Research Letters*, *45*, 2590–2596. <http://doi.org/10.1002/2018GL077312>
- Damiano, P. A., Delamere, P. A., Stauffer, B., Ng, C. S., & Johnson, J. R. (2019). Kinetic simulations of electron acceleration by dispersive scale Alfvén waves in Jupiter's magnetosphere. *Geophysical Research Letters*, *46*, 3043–3051. <https://doi.org/10.1029/2018GL081219>
- Delamere, P. A., Bagenal, F., Ergun, R., & Su, Y. J. (2003). Momentum transfer between the Io plasma wake and Jupiter's ionosphere. *Journal of Geophysical Research*, *108*(A6), 1241. <https://doi.org/10.1029/2002JA009530>
- Ergun, R. E., Ray, L., Delamere, P. A., Bagenal, F., Dols, V., & Su, Y. J. (2009). Generation of parallel electric fields in the Jupiter-Io torus wake region. *Journal of Geophysical Research*, *114*, A05201. <https://doi.org/10.1029/2008JA013968>
- Gérard, J., Bonfond, B., Grodent, D., Radioti, A., Clarke, J. T., Gladstone, G. R., et al. (2014). Hubble spectral observations, 9072–9088. *Journal of Geophysical Research: Space Physics*, *119*, 9072–9088. <https://doi.org/10.1002/2014JA020514>
- Gérard, J. C., Bonfond, B., Grodent, D., & Radioti, A. (2016). The color ratio-intensity relation in the Jovian aurora: Hubble observations of auroral components. *Planetary and Space Science*, *131*, 14–23. <https://doi.org/10.1016/j.pss.2016.06.004>
- Gérard, J. C., Bonfond, B., Mauk, B. H., Gladstone, G. R., Yao, Z. H., Greathouse, T. K., et al. (2019). Contemporaneous observations of Jovian energetic auroral electrons and ultraviolet emissions by the Juno spacecraft. *Journal of Geophysical Research: Space Physics*, *124*, 8298–8317. <https://doi.org/10.1029/2019JA026862>
- Gershman, D. J., Connerney, J. E. P., Kotsiaros, S., DiBaccio, G. A., Martos, Y. M., Viñas, A. F., et al. (2019). Alfvénic fluctuations associated with Jupiter's auroral emissions. *Geophysical Research Letters*, *46*, 7157–7165. <https://doi.org/10.1029/2019GL082951>

- Gladstone, G. R., Persyn, S. C., Eterno, J. S., Walther, B. C., Slater, D. C., Davis, M. W., et al. (2017). The ultraviolet spectrograph on NASA's Juno Mission. *Space Science Reviews*, *213*(1–4), 447–473. <https://doi.org/10.1007/s11214-014-0040-z>
- Grodent, D., Bonfond, B., Gérard, J. C., Radioti, A., Gustin, J., Clarke, J. T., et al. (2008). Auroral evidence of a localized magnetic anomaly in Jupiter's northern hemisphere. *Journal of Geophysical Research*, *113*, A09201. <https://doi.org/10.1029/2008JA013185>
- Grodent, D., Gérard, J. C., Gustin, J., Mauk, B. H., Connerney, J. E. P., & Clarke, J. T. (2006). Europa's FUV auroral tail on Jupiter. *Geophysical Research Letters*, *33*, L06201. <https://doi.org/10.1029/2005GL025487>
- Gustin, J., Gérard, J. C., Grodent, D., Gladstone, G. R., Clarke, J. T., Pryor, W. R., et al. (2013). Effects of methane on giant planet's UV emissions and implications for the auroral characteristics. *Journal of Molecular Spectroscopy*, *291*, 108–117. <https://doi.org/10.1016/j.jms.2013.03.010>
- Gustin, J., Grodent, D., Gérard, J. C., & Clarke, J. T. (2002). Spatially resolved far ultraviolet spectroscopy of the Jovian aurora. *Icarus*, *157*(1), 91–103. <https://doi.org/10.1006/icar.2001.6784>
- Gustin, J., Grodent, D., Ray, L. C., Bonfond, B., Bunce, E. J., Nichols, J. D., & Ozak, N. (2016). Characteristics of north Jovian aurora from STIS FUV spectral images. *Icarus*, *268*, 215–241. <https://doi.org/10.1016/j.icarus.2015.12.048>
- Hess, S. L. G., Delamere, P. A., Dols, V., Bonfond, B., & Swift, D. (2010). Power transmission and particle acceleration along the Io flux tube. *Journal of Geophysical Research*, *115*, A06205. <https://doi.org/10.1029/2009JA014928>
- Hess, S. L. G., Delamere, P. A., Dols, V., & Ray, L. C. (2011). Comparative study of the power transferred from satellite-magnetosphere interactions to auroral emissions. *Journal of Geophysical Research*, *116*, A01202. <https://doi.org/10.1029/2010JA015807>
- Hinton, P. C., Bagenal, F., & Bonfond, B. (2019). Alfvén wave propagation in the Io plasma torus. *Geophysical Research Letters*, *46*, 1242–1249. <https://doi.org/10.1029/2018GL081472>
- Kurth, W. S., Hospodarsky, G. B., Kirchner, D. L., Mokryzcki, B. T., Averkamp, T. F., Robison, W. T., et al. (2017). The Juno waves investigation. *Space Science Reviews*, *213*(1–4), 347–392. <https://doi.org/10.1007/s11214-017-0396-y>
- Mauk, B. H., Haggerty, D. K., Jaskulek, S. E., Schlemm, C. E., Brown, L. E., Cooper, S. A., et al. (2017). The Jupiter Energetic Particle Detector Instrument (JEDI) investigation for the Juno Mission. *Space Science Reviews*, *213*(1–4), 289–346. <https://doi.org/10.1007/s11214-013-0025-3>
- Mauk, B. H., Haggerty, D. K., Paranicas, C., Clark, G., Kollmann, P., Rymer, A. M., et al. (2017a). Juno observations of energetic charged particles over Jupiter's polar regions: Analysis of monodirectional and bidirectional electron beams. *Geophysical Research Letters*, *44*, 4410–4418. <https://doi.org/10.1002/2016GL072286>
- Mauk, B. H., Haggerty, D. K., Paranicas, C., Clark, G., Kollmann, P., Rymer, A. M., et al. (2017b). Discrete and broadband electron acceleration in Jupiter's powerful aurora. *Nature*, *549*(7670), 66–69. <https://doi.org/10.1038/nature23648>
- McComas, D. J. J., Alexander, N., Allegrini, F., Bagenal, F., Beebe, C., Clark, G., et al. (2017). The Jovian Auroral Distributions Experiment (JADE) on the Juno Mission to Jupiter. *Space Science Reviews*, *213*(1–4), 547–643. <https://doi.org/10.1007/s11214-013-9990-9>
- Neubauer, F. M. (1998). The sub-Alfvénic interaction of the Galilean satellites with the Jovian magnetosphere. *Journal of Geophysical Research*, *103*(E9), 19843–19866. <https://doi.org/10.1029/97JE03370>
- Paranicas, C., Mauk, B. H., Haggerty, D. K., Clark, G., Kollmann, P., Rymer, A. M., et al. (2019). Io's effect on energetic charged particles as seen in Juno data. *Geophysical Research Letters*, *46*, 13,615–13,620. <https://doi.org/10.1029/2019GL085393>
- Saur, J., Grambusch, T., Duling, S., Neubauer, F. M., & Simon, S. (2013). Magnetic energy fluxes in sub-Alfvénic planet star and moon planet interactions. *Astronomy and Astrophysics*, *552*, 1–20. <https://doi.org/10.1051/0004-6361/201118179>
- Saur, J., Janser, S., Schreiner, A., Clark, G., Mauk, B. H., Kollmann, P., et al. (2018). Wave-particle interaction of Alfvén waves in Jupiter's magnetosphere: Auroral and magnetospheric particle acceleration. *Journal of Geophysical Research: Space Physics*, *123*, 9560–9573. <https://doi.org/10.1029/2018JA025948>
- Saur, J., Strobel, D. F., & Neubauer, F. M. (1998). Interaction of the Jovian magnetosphere with Europa: Constraints on the neutral atmosphere. *Journal of Geophysical Research*, *103*(E9), 19,947–19,962. <https://doi.org/10.1029/97JE03556>
- Sulaiman, A. H., Hospodarsky, G. B., Elliott, S. S., Kurth, W. S., Gurnett, D. A., Imai, M., et al. (2020). Cross-scale wave-particle interactions associated with Io's footprint tail aurora: Evidence of Alfvén, ion cyclotron, and whistler modes. *Geophysical Research Letters*, *47*, e2020GL088432. <https://doi.org/10.1029/2020GL088432>
- Szalay, J. R., Allegrini, F., Bagenal, F., Bolton, S. J., Bonfond, B., Clark, G., et al. (2020a). Alfvénic acceleration sustains Ganymede's footprint tail aurora. *Geophysical Research Letters*, *47*, e2019GL086527. <https://doi.org/10.1029/2019GL086527>
- Szalay, J. R., Allegrini, F., Bagenal, F., Bolton, S. J., Bonfond, B., Clark, G., et al. (2020b). A new framework to explain changes in Io's footprint tail electron fluxes. *Geophysical Research Letters*, *47*, e2020GL089267. <https://doi.org/10.1029/2020GL089267>
- Szalay, J. R., Bagenal, F., Allegrini, F., Bonfond, B., Clark, G., Connerney, J. E. P., et al. (2020). Proton acceleration by Io's Alfvénic interaction. *Journal of Geophysical Research: Space Physics*, *125*, e27314. <https://doi.org/10.1029/2019JA027314>
- Szalay, J. R., Bonfond, B., Allegrini, F., Bagenal, F., Bolton, S., Clark, G., et al. (2018). In situ observations connected to the Io footprint tail aurora. *Journal of Geophysical Research: Planets*, *123*, 3061–3077. <https://doi.org/10.1029/2018JE005752>
- Zarka, P. (2007). Plasma interactions of exoplanets with their parent star and associated radio emissions. *Planetary and Space Science*, *55*(5), 598–617. <https://doi.org/10.1016/j.pss.2006.05.045>